Construction and Building Materials 306 (2021) 124839

Contents lists available at ScienceDirect

Construction and Building Materials

journal homepage: www.elsevier.com/locate/conbuildmat

Four-years influence of waste brick powder addition in the pore structure and several durability-related parameters of cement-based mortars

Rosa María Tremiño [a], Teresa Real-Herraiz [b], Viviana Letelier [c], José Marcos Ortega [a,*]

[a] Departamento de Ingeniería Civil, Universidad de Alicante, Ap. Correos 99, 03080 Alacant/Alicante, Spain
[b] Instituto de Matemática Multidisciplinar, Universidad Politécnica de Valencia, Camino de Vera s/n, 46022 Valencia, Spain
[c] Departamento de Obras Civiles, Universidad de la Frontera, Av. Fco. Salazar 01145, Temuco, Chile

ARTICLE INFO

Keywords:
Waste brick powder
Microstructure
Durability
Very long term
Sustainability
Additions

ABSTRACT

The service life of real construction elements is usually long, so the study of the behavior of cement-based materials with new pozzolanic additions in the very long term, after several hardening years, could be interesting. Here, the influence of using waste brick powder as 10% and 20% clinker substitution in microstructure and several durability-related parameters of mortars after 1500 hardening days (approximately 4 years) has been studied. According to the results obtained, the incorporation of brick powder overall improved the performance of mortars after 4 years, compared to reference mortars without addition, especially regarding the pore structure and chloride diffusion.

1. Introduction

To lessen the greenhouse gases emissions of the most pollutant sectors is today an important topic of study [1–4]. In this line, the industry of cement production has developed strategies for contributing to reach the present worldwide aims regarding the global warming reduction. One of the most popular strategies is to look for more sustainable cement-based materials, such as substituting partially or totally clinker by additions [5–7]. On one hand, it is interesting to highlight the classical additions, such as silica fume, ground granulated blast-furnace slag and fly ash [8–12], whose use has been become widespread in the last decades. On the other hand, the research of alternatives to the above-mentioned classical additions is now an important topic of research. These alternatives could be particularly useful for substituting fly ash, whose production will be considerably reduced in the near future, caused by the next closing or transformation of the coal-fired power stations, also regarding the current worldwide sustainable development goals. Several examples of these new additions are brick powder [13], rice hush ash [14], red mud [15], among others.

In relation to the use in cement-based materials of brick powder, coming from demolition residues and faulty bricks turned down from ceramic industry, several works [13,16–18] has studied its effects in the short term. In addition, it has been reported [13,16,19–22] the pozzolanic activity of brick powder, due to the transformation of crystalline structures of clay silicates in amorphous compounds produced by the exposure to high temperature during the bricks production [23]. In this regard, the work of Navrátilová et al. [13] particularly assessed the pozzolanic activity of brick powder with different methods, such as differential thermal analyses, determining the pozzolanic activity index with the modified Chapelle test and calculating another pozzolanic activity index from compressive strength, obtaining similar results with all of them, which revealed the pozzolanic character of brick powder. Additionally, Pereira-de-Oliveira et al. [16] evaluated the pozzolanic activity by a strength activity index for mortars with red-clay ceramic waste, also obtaining similar results.

On the other hand, several researches [17,24–26] showed that a maximum 20% substitution of clinker by brick powder could be adequate, without producing noticeable harmful effects in the properties of mortars and concretes, particularly in their mechanical performance. The possible filler effect of brick powder has also been reported [18] as a factor which could produce beneficial effects in cement-based materials with this addition. Furthermore, regarding the optimum particle size of this brick powder [27] for being used as clinker replacement, it has been determined that sizes lower than 0.06 mm would be recommended [28].

As has been previously explained, it is interesting to underline that most of existing research has studied the influence of brick powder at relatively short hardening ages [13,16–18]. However, the required service life of real construction elements, which belong to buildings,

* Corresponding author.
E-mail address: jm.ortega@ua.es (J.M. Ortega).

https://doi.org/10.1016/j.conbuildmat.2021.124839
Received 3 April 2021; Received in revised form 31 August 2021; Accepted 4 September 2021
Available online 13 September 2021

structures and other engineering works, is usually long [29]. Then, for evaluating if the new additions, such as brick powder, are adequate for being used in these real construction elements, it would be necessary to characterize their behaviour in the very long term, after hardening periods of several years. In addition, this could be especially relevant for pozzolanic materials.

Therefore, the main aim of this work is to analyze the influence of the use of brick powder as supplementary cementitious material, in the pore structure and several durability-related parameters of mortars after approximately 4 hardening years (1500 days). Mortars made with ordinary Portland cement without addition have been taken as reference. The studied percentages of clinker substitution by brick powder were 10% and 20%. The microstructure of the mortars was assessed with the non-destructive impedance spectroscopy technique and mercury intrusion porosimetry. In order to evaluate the development of the pozzolanic activity of the brick powder at the end of the 4 years time period studied, differential thermal analysis was performed, as well as X-ray diffraction and X-ray fluorescence. The durability-related parameters analyzed were the water absorption after immersion and the steady-state diffusion coefficient obtained from saturated sample's resistivity. Lastly, the possible development of shrinkage or expansion in the mortars was checked at the end of the studied time period.

2. Experimental setup

2.1. Materials and sample preparation

The brick powder (BP) studied in this work came from industrial brick residuals from demolition debris. In this work, the waste brick powder was sifted and only particles under 75 μm were taken for being used as addition. The chemical composition of the brick powder determined by X-ray fluorescence (XRF) is shown in Table 1. Its Blaine surface area [30] was 6485 m^2/kg. The inorganic crystalline phases present in the brick powder were silica, illite and hematite [31]. The particle size distribution of this addition, obtained using a high resolution laser particle size analyzer model Saturn DigiSizer 5200 manufactured by Micromeritics (Norcross, Georgia, USA), is depicted in Fig. 1.

Three types of mortars were prepared, combining waste brick powder and an ordinary Portland cement CEM I 42.5 R [32]. First of all, reference mortars with only cement CEM I 42.5 R and without brick powder were made, being designed as REF in the figures of the results section. In addition to this, mortars with two different contents of brick powder in the binder were also prepared. Those mortars included 10% and 20% in weight as a replacement of the ordinary Portland cement. They were named BP10 and BP20, respectively. The water to cement ratio was 0.5 and the aggregate to cement ratio was 3:1 for all the studied mortars. The aggregates consisted of fine quartz sand which accomplished the prescriptions of standard UNE-EN 196-1 [33] and it was provided by the company Normensand [34–36].

Two types of specimens were prepared. Firstly, cylinders with 10 cm diameter and 15 cm height were made. Moreover, prisms with sizes 25 mm × 25 mm × 285 mm were prepared too. Before de-moulding, all the abovementioned specimens were kept in a chamber at 20 °C and 95% relative humidity (RH) during the first 24 h from setting. Once finished that time period and de-moulded, cylinders were cut for obtaining disks with 1 cm height. Lastly, all the specimens were kept under a standard optimum laboratory condition (20 °C and 100% RH) up to approximately 4 years hardening (1500 days), when the different tests were performed.

Table 1
Chemical composition of waste brick powder determined by XRF.

Composition	Brick powder
Al_2O_3	39.05%
Fe_2O_3	12.73%
CaO	0.63%
SiO_2	41.47%
CuO	0.70%
TiO_2	1.03%
K_2O	2.81%
SO_3	1.59%

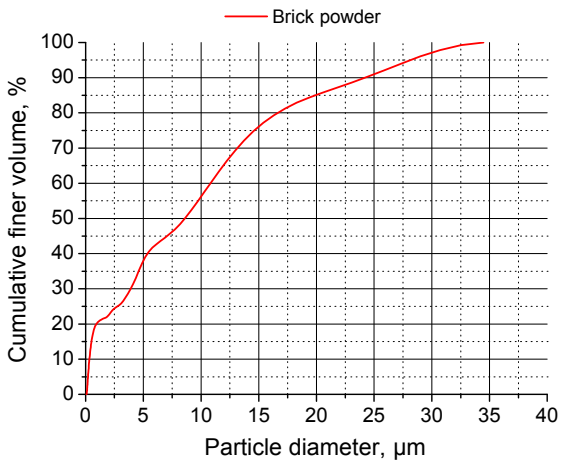

Fig. 1. Particle size distribution of waste brick powder obtained with a laser particle size analyzer.

2.2. Mercury intrusion porosimetry

The mercury intrusion porosimetry technique has been used for characterizing the microstructure of the mortars [37,38]. The porosimeter used was a Poremaster-60 GT model manufactured by Quantachrome Instruments (Boynton Beach, Florida, USA). The samples were oven-dried at 50 °C for 48 h prior to the test. The results analyzed in this work were total porosity, pore size distribution and percentage of Hg retained at the end of the experiment. In relation to the study of the Hg retained inside the solid specimen once finished the mercury intrusion porosimetry test, several authors have reported that this parameter is helpful to provide information on the pore tortuosity and connectivity of the porous network [39,40], and particularly this Hg volume entrapped is closely correlated to large pores connected through small mouth [41]. Finally, two measurements were performed on each binder at the age studied.

2.3. Impedance spectroscopy

The impedance spectroscopy technique also allows obtaining information about the pore structure of cementitious materials [42–44]. Here, this technique was performed using an impedance analyzer Agilent 4294A model (Agilent Technologies, Kobe, Japan), which permits capacitance measurements ranged between 10^{-14}F and 0.1F, being 10^{-15}F its maximum resolution. The electrodes used were circular ante their diameter was 8 cm. They were made with a flexible graphite sheet attached to a disk of copper, which had the abovementioned diameter. The frequency range was from 100 Hz to 100 MHz.

Contacting and non-contacting measurement methods were used [42], fitting the experimental data to the equivalent circuits proposed by Cabeza et al. [42]. Their components are several resistances and capacitances. In those circuits, the resistance R_1 is particularly related to the percolating pores in the sample [42]. Then, it could be expected higher values of this parameter when the volume of percolating porosity of the specimens decreases, due to development of hydration and pozzolanic reactions, because the products of these reactions would progressively close the pore paths which cross the sample. The resistance R_2 gives data about the pores in general [42] and several works

[45,46] have pointed out that greater values of this parameter are related to the higher presence of finer pores in the material.

On the other hand, the capacitance C_1 provides information regarding the solid fraction of the specimens [42], so it is expected that this parameter increases as solid formation is produced due to the development of hydration and pozzolanic reactions [47]. The capacitance C_2 is associated with the surface of the pores in contact with the electrolyte that fills the pore network of the material [43]. This parameter is related to the formation of CSH gel layers, which occupy the pores [43] and it has been shown to be very sensitive to the variations of the amount of water in the pores [47,48]. The solid phases produced during the hydration and pozzolanic reactions are deposited on the pore surface and they increase the specific surface of the pores, because these products form rough structures [47], rising the values of capacitance C_2.

In this research, only the values of the parameters R_2, C_1 and C_2 obtained with the non-contacting method were analyzed in relation to the pore structure characterization, due to their greater accuracy. The resistance R_1, which can be only obtained using the contacting method, was only used for calculating the steady-state chloride diffusion coefficient in water saturated specimens, as will be explained in subsection 2.6. Eight different disks of 1 cm height were tested with this technique for each mortar type.

2.4. Differential thermal analysis

The differential thermal analyses were performed using a simultaneous TG-DTA model TGA/SDTA851e/SF/1100 from Mettler Toledo, which allows working from room temperature to 1100 °C. The heating ramp selected was 20 °C/min up to 1000 °C in N_2 atmosphere. The curve weight derivate versus temperature was determined for each mortar type.

2.5. X-ray diffraction (XRD) and X-ray fluorescence (XRF)

X-ray diffractions were performed using a Bruker D8 Advance difractometer (Bruker Española S.A., Madrid, Spain). The spectrum was registered with stepping intervals from 4° to 60° at 0.05° in the Θ- Θ mode (X-ray tube power: 40 kV and 40 mA). X-ray spectra were obtained for each mortar type after 1500 hardening days. In addition, at the abovementioned age, the chemical composition of the mortars was determined with X-ray fluorescence, using an X-ray sequential spectrometer model Philips Magix Pro PW2400.

2.6. Steady-state diffusion coefficient

The steady-state chloride diffusion coefficient has been calculated from the electrical resistivity of the saturated samples. The resistivity was obtained from the resistance R_1 of impedance spectroscopy technique, determined in water saturated samples. As has been explained in section 2.3, the impedance resistance R_1 is directly related to the percolating pores of the specimens [42], being then equivalent to their electrical resistance [49]. For each mortar type, six different disks of 1 cm height were tested. Lastly, the steady-state diffusion coefficient was determined with the next equation [50]:

$$D_S = \frac{2 \times 10^{-10}}{\rho} \quad (1)$$

in which: D_s is the chloride steady-state diffusion coefficient through the sample (m^2/s) and ρ is the electrical resistivity of the specimen (Ω·m).

2.7. Water absorption

The absorption after immersion was determined according to the procedure described in the ASTM Standard C642-06 [51]. Six pieces taken from slices of 1 cm thickness were tested for each kind of mortar studied.

2.8. Expansion/shrinkage

For evaluating the possible effects of waste brick powder addition regarding the expansion or shrinkage in the mortars, their length change was determined after 1500 hardening days. For each binder, six prisms with dimensions 25 mm × 25 mm × 285 mm were tested. The length change in percentage respect to initial length was obtained from the measurements made using a length comparator [52].

3. Results

3.1. Mercury intrusion porosimetry

The results of total porosity obtained for REF, BP10 and BP20 series at 1500 hardening days can be observed in Fig. 2. It has been noted scarce differences between the types of mortar studied. Despite that, this parameter was slight higher for BP20 series and scarce smaller for BP10 ones, in comparison with reference mortars without addition.

The pore size distributions of the analyzed mortars are depicted in Fig. 3. As can be observed, specimens with brick powder showed higher percentages of pores with lower diameters, especially for those in the range < 10 nm, compared to reference series. In addition, the proportion of those finer pores increased as higher was the content of brick powder in the material. Then, the incorporation of brick powder in the binder entailed a noticeable microstructure refinement of the mortars after approximately 4 hardening years.

The percentages of mercury retained at the end porosimetry test are represented in Fig. 4. Mortars with brick powder showed higher values of this parameter in comparison with REF ones.

3.2. Impedance spectroscopy

The impedance capacitance C_1 results are depicted in Fig. 5. This parameter was relatively similar for the analyzed mortars series, although samples with brick powder showed slight higher capacitance C_1 than reference ones at the studied age.

The results of impedance capacitance C_2 are shown in Fig. 6. Mortars with brick powder presented noticeable greater values of this capacitance, compared to those without addition. Furthermore, this parameter was higher for BP20 samples than for BP10 ones.

Regarding the resistance R_2, the results noted for this parameter are represented in Fig. 7. The resistance R_2 was significantly higher for samples with brick powder, in comparison with REF series. In addition, this parameter increased as the percentage of brick powder in the binder rose, showing BP20 mortars the highest R_2 values.

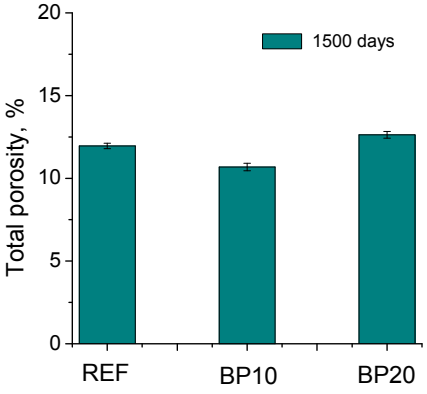

Fig. 2. Results of total porosity noted for the studied mortars. Error bars in this figure and in the following represents the standard deviation.

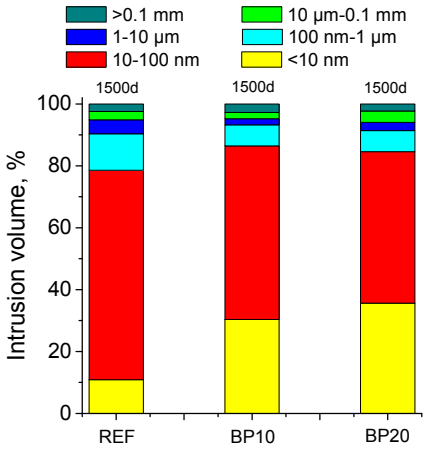

Fig. 3. Pore size distributions obtained for the analyzed mortar series.

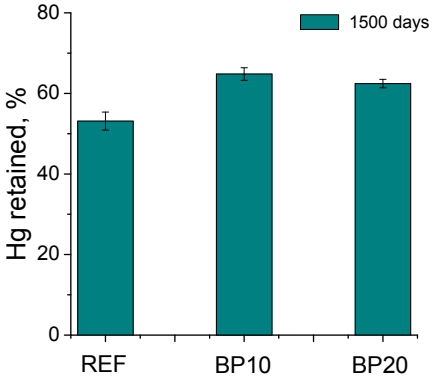

Fig. 4. Results of percentage of mercury retained at the end of porosimetry noted for REF, BP10 and BP20 series.

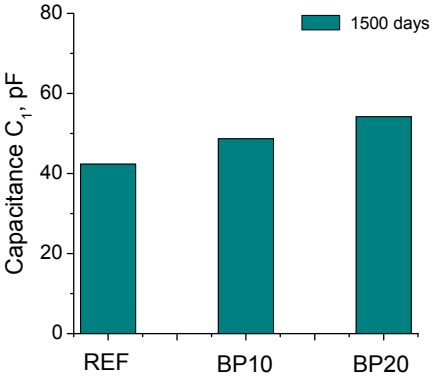

Fig. 5. Capacitance C_1 results for the studied series.

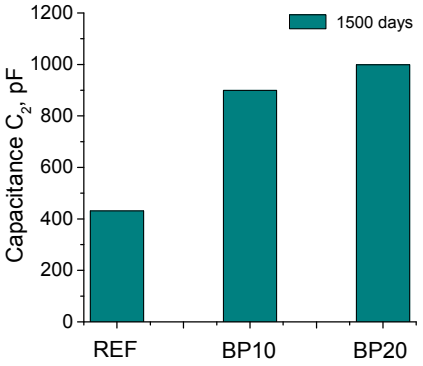

Fig. 6. Results of capacitance C_2 obtained for the types of mortars studied.

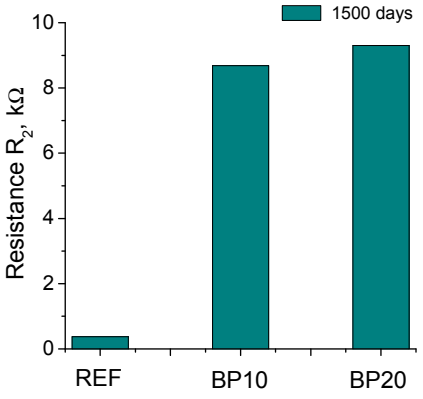

Fig. 7. Resistance R_2 results noted for REF, BP10 and BP20 mortars.

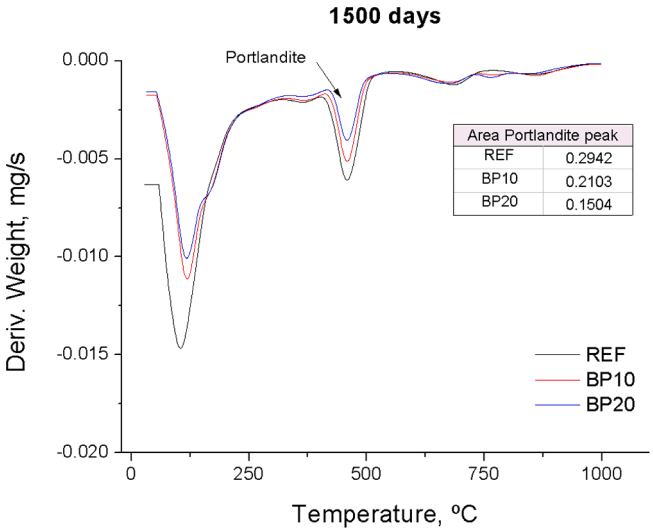

Fig. 8. Derivate of weight versus temperature curve obtained for the studied mortars at 1500 hardening days.

3.3. *Differential thermal analysis (DTA)*

The derivate of weight versus temperature curves obtained for the REF, BP10 and BP20 at 1500 hardening ages are shown in Fig. 8. As can be observed, the portlandite peak area of this curve was lower as rose the proportion of brick powder in the binder.

3.4. *X-ray diffraction (XRD) and X-ray fluorescence (XRF) analyses*

The X-ray spectra obtained for REF, BP10 and BP20 mortars are represented in Fig. 9a–c, respectively. As can be observed, a reduction of the peak intensities of portlandite was produced as increase the content of brick powder in the binder, in agreement with DTA data. The XRF results for the studied mortars are shown in Table 2. The main components of the mortars were CaO, SiO_2 and Al_2O_3. The addition of brick powder produced an increase of percentage of Al_2O_3 and SiO_2 in the mortars, whereas it reduced the percentage of CaO.

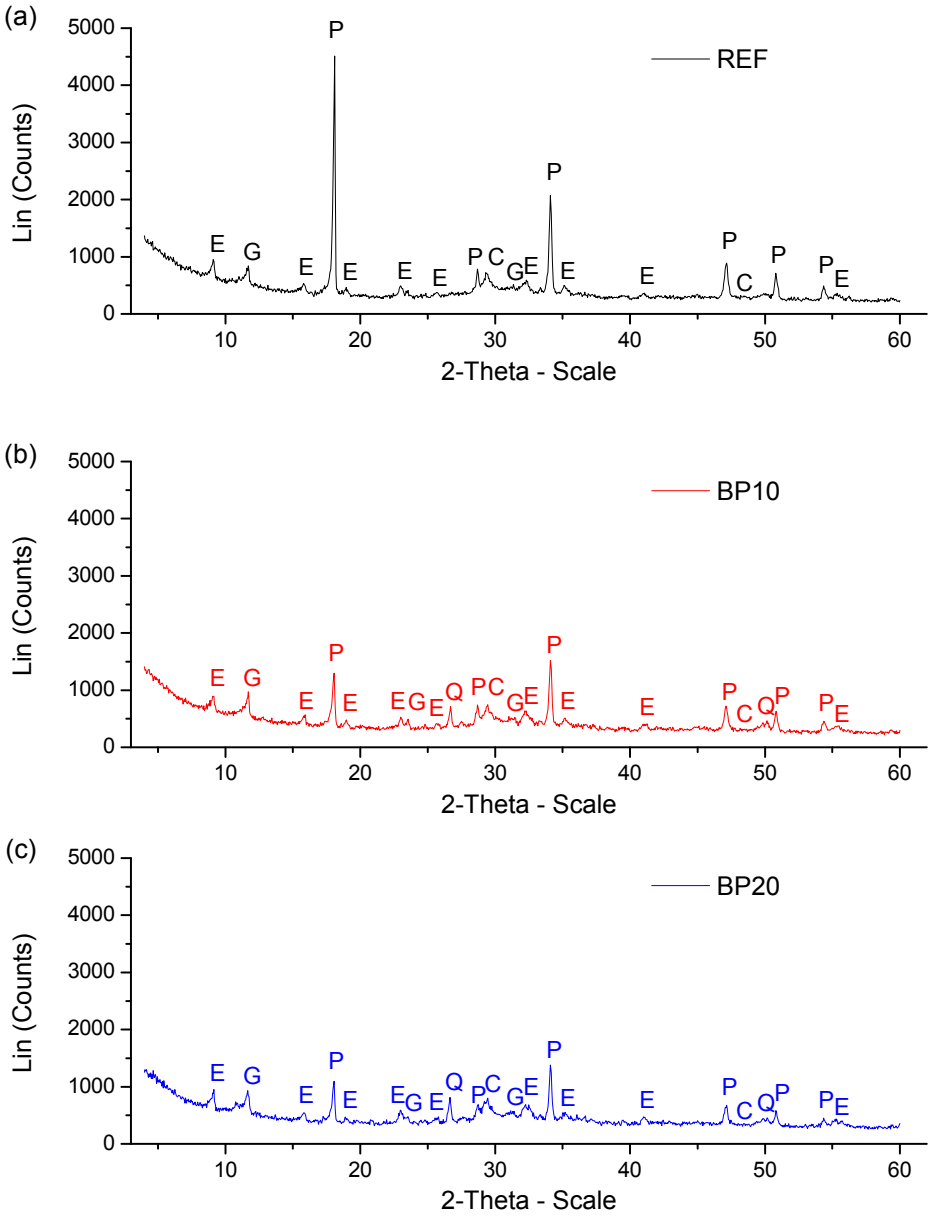

Fig. 9. (a) XRD spectrum for REF mortars; (b) XRD spectrum for BP10 mortars; (c) XRD spectrum for BP20 mortars. The meaning of the letters in the figure is the following: P Portlandite, C Calcite, E Ettringite, G Gypsum, Q Quartz.

Table 2
X-ray fluorescence results for REF, BP10 and BP20 mortars after 1500 hardening days.

Composition	REF (%)	BP10 (%)	BP20 (%)
Na_2O	0.25	0.25	0.3
MgO	1.36	1.38	1.35
Al_2O_3	4.66	6.73	8.75
SiO_2	17.07	20.07	22.31
P_2O_5	0.18	0.19	0.17
SO_3	3.94	3.07	3.51
K_2O	0.91	1.33	1.96
CaO	68.28	62.66	56.61
TiO_2	0.39	0.53	0.64
Fe_2O_3	2.63	3.39	3.90
Other elements	<0.33	<0.4	<0.5

3.5. Steady-state chloride diffusion coefficient

The results of steady-state chloride diffusion coefficient obtained from sample's resistivity at 1500 hardening days are represented in Fig. 10. The lowest values of this coefficient were noted for BP20 mortars, followed by BP10 ones. On the other hand, the highest diffusion coefficient was observed for reference specimens without addition of brick powder.

3.6. Water absorption

The results of percentage of water absorption after immersion [51] are depicted in Fig. 11. At 1500 hardening days, this parameter was relatively similar for the different binders studied. Specimens with brick powder showed slightly higher percentage of water absorption after immersion compared to reference ones, despite that in any case the differences between the series studied were not noticeable.

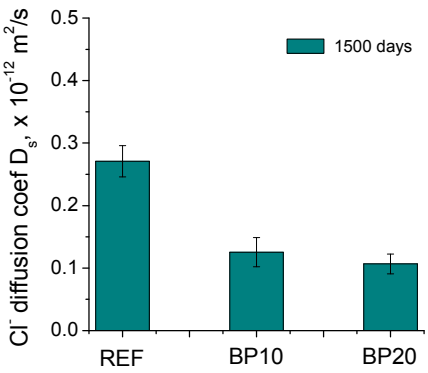

Fig. 10. Results of steady-state chloride diffusion coefficient obtained from sample's resistivity noted for the analyzed mortars series.

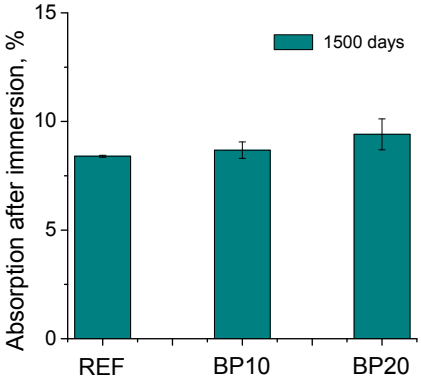

Fig. 11. Results of absorption after immersion [39] noted for the studied mortars.

3.7. Expansion/shrinkage

The percentage of length change respect to the initial length obtained for REF, BP10 and BP20 series at 1500 hardening days is depicted in Fig. 12. All the series developed expansion along the period of time studied. Reference mortars showed higher expansion, whereas it was lower as increased the percentage of brick powder in the binder.

4. Discussion

4.1. Microstructure characterization

Regarding the results obtained using mercury intrusion porosimetry,

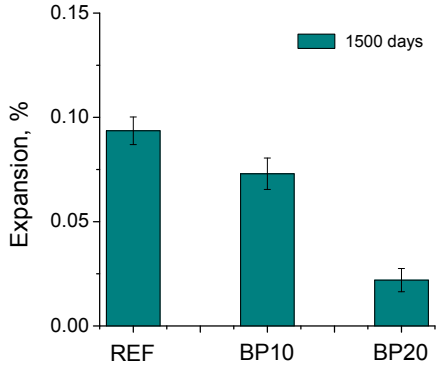

Fig. 12. Percentage of length change (expansion) obtained for the analyzed series after 1500 hardening days.

the total porosity was relatively similar at 1500 hardening days for all the analyzed mortar series (see Fig. 2). This result would indicate that in general the solid fraction and the global volume of pores was similar in the mortars, with independence of the binder. In view of that, the addition of waste brick powder up to 20% of the binder would not produce harmful effects in the very long term regarding the porosity of the mortars, in comparison with samples without this addition. However, the pore size distributions noted after 1500 hardening days showed that the incorporation of waste brick powder would produce a higher microstructure refinement, highlighting the greater proportion of pores with diameters in the range < 10 nm in BP10 and BP20 mortars in comparison with REF ones (see Fig. 3). The percentage of Hg retained at the end porosimetry test (see Fig. 4) was higher for mortars with waste brick powder. As has been previously explained, this parameter provides qualitatively information related to the pores tortuosity [40,41]. Therefore, the results of Hg retained would indicate a greater pore network tortuosity for samples with waste brick powder at the studied age, also suggesting a higher pore refinement produced by this addition.

The impedance spectroscopy results presented similarities with those observed using mercury intrusion porosimetry, already discussed. Firstly, the impedance capacitance C_1 provides information about the global solid fraction in the sample [42], independently of its pore size distribution. This capacitance was slightly higher for BP mortars, although the differences between the different binders studied were small (see Fig. 5). This would indicate that there were scarce differences in the global solid fraction of the analyzed mortars at the end of studied hardening time period. The capacitance C_1 results would be in keeping with total porosity ones, which also suggest low differences in overall pores volume, independently of the incorporation of brick powder. The small influence in the global porosity produced by the addition of brick powder, while a pore network refinement was produced, have been also observed for other additions, for example fly ash [53].

The impedance capacitance C_2 is related to the internal surface of the pores in contact with the electrolyte that fills the pore structure of the material [43]. The increase of this surface could be caused by the formation of new solid phases, as products of the hydration and pozzolanic reactions. These solids would form new rough structures on the already existing pore walls, producing a progressive refinement of the microstructure and increasing in this way the capacitance C_2 [47]. This parameter was greater for mortars with waste brick powder after 1500 hardening days, in comparison with mortars without this addition. Furthermore, the capacitance C_2 increased as higher was the content of brick powder in the sample (see Fig. 6). In view of these results, the internal surface of the pores would be higher for samples with brick powder compared to reference ones. This would indicate that the incorporation of waste brick powder would produce a higher pore refinement in the mortars in the very long term, being in agreement with the results of pore size distributions and percentage of Hg retained, obtained with mercury intrusion porosimetry.

On the other hand, the impedance resistance R_2 provides data related to the pore network of the material [43]. In general, greater resistances R_2 would reveal a higher presence of finer pores. In this work, higher values of this parameter were noted for brick powder mortars compared to reference specimens (see Fig. 7). Moreover, the resistance R_2 rose as increased the content of this addition in the sample. These would agree with the results noted for capacitance C_2, pore size distributions and Hg retained, suggesting the refinement of the microstructure produced in the very long term by this supplementary cementitious material.

The finer microstructure of brick powder mortars after 1500 hardening days revealed by the characterization performed by mercury intrusion porosimetry and impedance spectroscopy could be mainly due to the pozzolanic activity of this addition [13,16]. New solids would be formed as products of pozzolanic reactions of brick powder, reducing the pore sizes and closing the microstructure. The results of the differential thermal analyses would also confirm this pozzolanic activity of the waste brick powder in the very long term, as suggested the lower

areas of portlandite peak in the curves derivate of weight versus temperature for brick powder series, compared to reference ones (see Fig. 8). Furthermore, the lower intensities of portlandite peaks for binders with brick powder obtained with XRD, would also reveal this pozzolanic activity in the very long term (see Fig. 9). This would be also in line with the reduction of the content of CaO in the mortars produced by the addition of brick powder, as well as with the higher presence of Al_2O_3 and SiO_2 in these mortars (see Table 2). These results would agree with other works [13,16,21] in which it has been assessed the possible pozzolanic activity of brick residues in the short term, using different parameters, such as pozzolanic activity index [13] and strength activity index [13,16]. Finally, in addition to the benefits of the pozzolanic reactions of brick powder in the microstructure development of the mortars, the filler effect of this addition could also contribute to the pore refinement observed after 1500 hardening days, as has been suggested by other authors [18].

4.2. Durability-related parameters

With regard to the studied durability-related parameters of the mortars, it is relevant to obtain information about the diffusion of chlorides in the very long term, because this aggressive ion is one of most damaging agents related to the corrosion of reinforcement elements embedded in cementititious materials. The mortars with waste brick powder showed lower steady-state chloride diffusion coefficients compared to reference ones (see Fig. 10). This result could be a consequence of the more refined microstructure of the specimens with waste brick powder, in comparison with those without this addition, produced by the pozzolanic reactions of brick powder [13] and its filler effect [18], as has been previously explained. The displacement of chlorides in the pore network of the material would be more complicated as the proportion of pores with smaller sizes is higher, giving as a result smaller diffusion coefficients, as been observed for brick powder mortars.

Slight differences have been noted regarding the percentage of absorption after immersion at 1500 hardening days between the different mortars studied (see Fig. 11). This result would agree with those obtained for total porosity and impedance spectroscopy capacitance C_1, which revealed a similar volume of pores and total solid fraction in the analyzed mortar series. In view of the results of length change percentage respect to initial length, it has been observed an expansion for all the analyzed mortars (see Fig. 12). This could be due to the storage of the specimens in an optimum laboratory condition along the time period studied, which facilitates the hydration of the materials. Despite that, the addition of waste brick powder produced lower expansion than that observed for specimens without this addition, being this result in keeping with those obtained by other authors [54].

Finally, in view of the abovementioned results, the replacement up to 20% of clinker by waste brick powder would improve the performance of the mortars after 1500 hardening days regarding the pore structure and the diffusion of chlorides. In addition to this, the incorporation of brick powder would not produce harmful effects regarding other parameters of the mortars, like the percentage of absorption by immersion and the overall porosity. These results at several hardening years of the material could be useful in order to get information about the possible application of waste brick powder in real construction elements, especially due to the long service life required to these elements [29].

5. Conclusions

The main conclusions that can be drawn from the results previously discussed can be summarized as follows:

- The mortars with brick powder showed a higher pore refinement at 1500 days compared to those without this addition, in view of the results of several parameters obtained with impedance spectroscopy (capacitance C_2 and resistance R_2) and mercury intrusion porosimetry (pore size distributions and percentage of Hg retained at the end of the test).
- The proportion of finer pores was greater as higher was the content of brick powder in the mortars. This refinement of the pore network due to the incorporation of brick powder could be mainly produced by its pozzolanic activity, as would confirm the XRD, XRF and differential thermal analyses performed at 1500 hardening days. Furthermore, the filler effect of the brick powder could also contribute to this pore refinement.
- After approximately 4 years, the results of total porosity and impedance capacitance C_1 revealed that the overall solid fraction and volume of pores in the mortars was very similar, independently of the content of brick powder.
- The incorporation of waste brick powder improved the steady-state chloride diffusion coefficient of the mortars at 1500 days. This better behaviour would be due to the higher pore refinement produced by the pozzolanic activity of this addition, in combination with its filler effect.
- The water absorption after immersion in the very long term was similar for all the mortars studied, which would suggest that their volume of pores would be also similar, being in keeping with total porosity and capacitance C_1 results.
- According to the results noted in this work, the addition of 10% and 20% of brick powder as clinker replacement, would overall improve the behaviour of mortars at approximately 4 hardening years, compared to those made with only ordinary Portland cement in the binder, especially regarding the pore structure and chloride diffusion.

CRediT authorship contribution statement

Rosa María Tremiño: Investigation, Data curation, Writing – original draft. **Teresa Real-Herraiz:** Methodology, Investigation, Supervision. **Viviana Letelier:** Conceptualization, Methodology, Writing - review & editing, Funding acquisition. **José Marcos Ortega:** Conceptualization, Methodology, Investigation, Data curation, Writing - review & editing, Supervision, Funding acquisition.

Declaration of Competing Interest

The authors declare that they have no known competing financial interests or personal relationships that could have appeared to influence the work reported in this paper.

Acknowledgments

Authors wish to thank Cementos Portland Valderrivas S.A. for providing the ordinary Portland cement used in this study. The results included in this paper have been obtained in the PhD thesis carried out by Rosa María Tremiño at University of Alicante (Spain), under the supervision of José Marcos Ortega and Teresa Real-Herraiz.

Funding

This work was supported by the Conselleria de Educación, Investigación, Cultura y Deporte (at present re-named as Conselleria de Innovación, Universidades, Ciencia y Sociedad Digital) de la Generalitat Valenciana (Spain) [grant number GV/2019/070]; and by the Agencia Nacional de Investigación y Desarrollo de Chile (ANID) [grant number FONDECYT REGULAR 1211135].

References

[1] E. Benhelal, E. Shamsaei, M.I. Rashid, Challenges against CO<inf>2</inf> abatement strategies in cement industry: a review, J. Environ. Sci. (China) 104 (2021) 84–101, https://doi.org/10.1016/j.jes.2020.11.020.

[2] C.-Y. Zhang, B. Yu, J.-M. Chen, Y.-M. Wei, Green transition pathways for cement industry in China, Resour. Conserv. Recycl. 166 (2021), https://doi.org/10.1016/j.resconrec.2020.105355.

[3] B.J. Sergi, P.J. Adams, P.J. Adams, N.Z. Muller, N.Z. Muller, N.Z. Muller, A. L. Robinson, A.L. Robinson, S.J. Davis, S.J. Davis, J.D. Marshall, I.L. Azevedo, Optimizing emissions reductions from the U.S. power sector for climate and health benefits, Environ. Sci. Technol. 54 (2020) 7513–7523, https://doi.org/10.1021/acs.est.9b06936.

[4] F. Akbari, A. Mahpour, M.R. Ahadi, Evaluation of energy consumption and CO<inf>2</inf> emission reduction policies for urban transport with system dynamics approach, Environ. Model. Assess. 25 (2020) 505–520, https://doi.org/10.1007/s10666-020-09695-w.

[5] Y. Liu, K.S. Sidhu, Z. Chen, E.-H. Yang, Alkali-treated incineration bottom ash as supplementary cementitious materials, Constr. Build. Mater. 179 (2018) 371–378, https://doi.org/10.1016/j.conbuildmat.2018.05.231.

[6] V. Corinaldesi, G. Moriconi, Influence of mineral additions on the performance of 100% recycled aggregate concrete, Constr. Build. Mater. 23 (8) (2009) 2869–2876, https://doi.org/10.1016/j.conbuildmat.2009.02.004.

[7] K.-H. Yang, Y.-B. Jung, M.-S. Cho, S.-H. Tae, Effect of supplementary cementitious materials on reduction of CO2 emissions from concrete, J. Clean. Prod. 103 (2015) 774–783, https://doi.org/10.1016/j.jclepro.2014.03.018.

[8] J. Mirza, M.S. Mirza, V. Roy, K. Saleh, Basic rheological and mechanical properties of high-volume fly ash grouts, Constr. Build. Mater. 16 (6) (2002) 353–363, https://doi.org/10.1016/S0950-0618(02)00026-0.

[9] S.T. Lee, H.Y. Moon, R.N. Swamy, Sulfate attack and role of silica fume in resisting strength loss, Cem. Concr. Compos. 27 (1) (2005) 65–76, https://doi.org/10.1016/j.cemconcomp.2003.11.003.

[10] M.D.A. Thomas, A. Scott, T. Bremner, A. Bilodeau, D. Day, Performance of slag concrete in marine environment, ACI Mater. J. 105 (2008) 628–634. http://www.scopus.com/inward/record.url?eid=2-s2.0-57149145850&partnerID=tZOtx3y1.

[11] J.M. Ortega, J.L. Pastor, A. Albaladejo, I. Sánchez, M.A. Climent, Durability and compressive strength of blast furnace slag-based cement grout for special geotechnical applications, Mater. Constr. 64 (2014), https://doi.org/10.3989/mc.2014.04912.

[12] J.M. Ortega, M.D. Esteban, R.R. Rodríguez, J.L. Pastor, F.J. Ibanco, I. Sánchez, M. A. Climent, Influence of silica fume addition in the long-term performance of sustainable cement grouts for micropiles exposed to a sulphate aggressive medium, Materials (Basel) 10 (2017), https://doi.org/10.3390/ma10080890.

[13] E. Navrátilová, P. Rovnaníková, Pozzolanic properties of brick powders and their effect on the properties of modified lime mortars, Constr. Build. Mater. 120 (2016) 530–539, https://doi.org/10.1016/j.conbuildmat.2016.05.062.

[14] W. Xu, T. Lo, W. Wang, D. Ouyang, P. Wang, F. Xing, Pozzolanic reactivity of silica fume and ground rice husk ash as reactive silica in a cementitious system: a comparative study, Materials 9 (3) (2016) 146, https://doi.org/10.3390/ma9030146.

[15] D.V. Ribeiro, J.A. Labrincha, M.R. Morelli, Potential use of natural red mud as pozzolan for Portland cement, Mater. Res. 14 (2011) 60–66, https://doi.org/10.1590/S1516-14392011005000001.

[16] L.A. Pereira-De-Oliveira, J.P. Castro-Gomes, P.M.S. Santos, The potential pozzolanic activity of glass and red-clay ceramic waste as cement mortars components, Constr. Build. Mater. 31 (2012) 197–203, https://doi.org/10.1016/j.conbuildmat.2011.12.110.

[17] J. Katzer, Strength performance comparison of mortars made with waste fine aggregate and ceramic fume, Constr. Build. Mater. 47 (2013) 1–6, https://doi.org/10.1016/j.conbuildmat.2013.04.039.

[18] A. Schackow, D. Stringari, L. Senff, S.L. Correia, A.M. Segadães, Influence of fired clay brick waste additions on the durability of mortars, Cem. Concr. Compos. 62 (2015) 82–89, https://doi.org/10.1016/j.cemconcomp.2015.04.019.

[19] H. Böke, S. Akkurt, B. İpekoğlu, E. Uğurlu, Characteristics of brick used as aggregate in historic brick-lime mortars and plasters, Cem. Concr. Res. 36 (6) (2006) 1115–1122, https://doi.org/10.1016/j.cemconres.2006.03.011.

[20] F. Puertas, A. Barba, M.F. Gazulla, M.P. Gómez, M. Palacios, S. Martínez-ramírez, Ceramic wastes as raw materials in portland cement clinker fabrication: Characterization and alkaline activation, Mater. Constr. 56 (2006) 73–84. https://www.scopus.com/inward/record.uri?eid=2-s2.0-33646259987&partnerID=40&md5=1efbc1f722fba7530b17bbb4383757c4.

[21] A. Naceri, M.C. Hamina, Use of waste brick as a partial replacement of cement in mortar, Waste Manage. 29 (8) (2009) 2378–2384, https://doi.org/10.1016/j.wasman.2009.03.026.

[22] T. Vieira, A. Alves, J. de Brito, J.R. Correia, R.V. Silva, Durability-related performance of concrete containing fine recycled aggregates from crushed bricks and sanitary ware, Mater. Des. 90 (2016) 767–776, https://doi.org/10.1016/j.matdes.2015.11.023.

[23] A.A. Aliabdo, A.-E. Abd-Elmoaty, H.H. Hassan, Utilization of crushed clay brick in concrete industry, Alexandria Eng. J. 53 (1) (2014) 151–168, https://doi.org/10.1016/j.aej.2013.12.003.

[24] T. Kulovaná, E. Vejmelková, M. Keppert, P. Rovnaníková, Z. Keršner, R. Černý, Mechanical, durability and hygrothermal properties of concrete produced using Portland cement-ceramic powder blends, Struct. Concr. 17 (2016) 105–115, https://doi.org/10.1002/suco.201500029.

[25] A.E. Lavat, M.A. Trezza, M. Poggi, Characterization of ceramic roof tile wastes as pozzolanic admixture, Waste Manage. 29 (5) (2009) 1666–1674, https://doi.org/10.1016/j.wasman.2008.10.019.

[26] Z. Ge, Z. Gao, R. Sun, L. Zheng, Mix design of concrete with recycled clay-brick-powder using the orthogonal design method, Constr. Build. Mater. 31 (2012) 289–293, https://doi.org/10.1016/j.conbuildmat.2012.01.002.

[27] Z. Ge, Y. Wang, R. Sun, X. Wu, Y. Guan, Influence of ground waste clay brick on properties of fresh and hardened concrete, Constr. Build. Mater. 98 (2015) 128–136, https://doi.org/10.1016/j.conbuildmat.2015.08.100.

[28] L. Zheng, Z. Ge, Z. Yao, Z. Gao, Mechanical properties of mortars with recycled clay-brick-powder, in: Proc. 11th Int. Conf. Chinese Transp. Prof. ICCTP 2011, American Society of Civil Engineers, Nanjing, China, n.d.: pp. 3379–3388.

[29] European committee for standardization, EN 1992-1-1 Eurocode 2: Design of concrete structures - Part 1-1: General rules and rules for buildings, Brussels, 2004.

[30] ASTM, ASTM C204-16 Standard Test Methods for Fineness of Hydraulic Cement by Air Permeability Apparatus, (2016) 10.

[31] V. Letelier, J.M. Ortega, P. Muñoz, E. Tarela, G. Moriconi, Influence of waste brick powder in the mechanical properties of recycled aggregate concrete, Sustainability 10 (2018), https://doi.org/10.3390/su10041037.

[32] AENOR, UNE-EN 197-1:2011. Composición, especificaciones y criterios de conformidad de los cementos comunes., (2000) 30.

[33] AENOR, UNE-EN 196-1:2005. Métodos de ensayo de cementos. Parte 1: Determinación de resistencias mecánicas, (2005).

[34] Normensand GmbH, Normensand, (2021). https://www.normensand.de/en/home/ (accessed March 20, 2021).

[35] Normensand GmbH, Material Information Sheet Normensand, (2017) 9. https://www.normensand.de/fileadmin/gruppen/Normensand/Downloads/2017-05-09_Normensand_Material-Information-Sheet.pdf (accessed March 20, 2021).

[36] Normensand GmbH, Untersuchungsbericht Normensand, (2020) 7. https://www.normensand.de/fileadmin/gruppen/Normensand/Downloads/Untersuchungsbericht_Gesamtstatistik.pdf (accessed March 20, 2021).

[37] Sidney Diamond, Mercury porosimetry, Cem. Concr. Res. 30 (10) (2000) 1517–1525, https://doi.org/10.1016/S0008-8846(00)00370-7.

[38] S. Ouellet, B. Bussière, M. Aubertin, M. Benzaazoua, Microstructural evolution of cemented paste backfill: Mercury intrusion porosimetry test results, 37 (2007) 1654–1665. 10.1016/j.cemconres.2007.08.016.

[39] B. Díaz, L. Freire, X.R. Nóvoa, M.C. Pérez, Chloride and CO<inf>2</inf> transport in cement paste containing red mud, Cem. Concr. Compos. 62 (2015) 178–186, https://doi.org/10.1016/j.cemconcomp.2015.02.011.

[40] B. Díaz, L. Freire, P. Merino, X.R. Nóvoa, M.C. Pérez, Impedance spectroscopy study of saturated mortar samples, Electrochim. Acta 53 (25) (2008) 7549–7555, https://doi.org/10.1016/j.electacta.2007.10.042.

[41] P.A. Webb, C. Orr, R.W. Camp, J.P. Olivier, Y.S. Yunes, Analytical Methods in Fine Particle Technology, 1st editio, Micromeritics Instrument Corporation, Norcross, USA, 1997.

[42] M. Cabeza, P. Merino, A. Miranda, X.R. Nóvoa, I. Sanchez, Impedance spectroscopy study of hardened Portland cement paste, Cem. Concr. Res. 32 (6) (2002) 881–891, https://doi.org/10.1016/S0008-8846(02)00720-2.

[43] M. Cabeza, M. Keddam, X.R. Nóvoa, I. Sánchez, H. Takenouti, Impedance spectroscopy to characterize the pore structure during the hardening process of Portland cement paste, Electrochim. Acta 51 (8-9) (2006) 1831–1841, https://doi.org/10.1016/j.electacta.2005.02.125.

[44] S.W. Tang, X.H. Cai, Z. He, W. Zhou, H.Y. Shao, Z.J. Li, T. Wu, E. Chen, The review of pore structure evaluation in cementitious materials by electrical methods, Constr. Build. Mater. 117 (2016) 273–284, https://doi.org/10.1016/j.conbuildmat.2016.05.037.

[45] J.M. Ortega, V. Letelier, M. Miró, G. Moriconi, M. Ángel Climent, I. Sánchez, Influence of waste glass powder addition on the pore structure and service properties of cement mortars, Sustainability 10 (2018), https://doi.org/10.3390/su10030842.

[46] J.L. Pastor, J.M. Ortega, M. Flor, M.P. López, I. Sánchez, M.A. Climent, Microstructure and durability of fly ash cement grouts for micropiles, Constr. Build. Mater. 117 (2016), https://doi.org/10.1016/j.conbuildmat.2016.04.154.

[47] J.M. Ortega, I. Sánchez, M.A. Climent, Impedance spectroscopy study of the effect of environmental conditions in the microstructure development of OPC and slag cement mortars, Arch. Civ. Mech. Eng. 15 (2015), https://doi.org/10.1016/j.acme.2014.06.002.

[48] M. Cabeza, P. Merino, X.R. Nóvoa, I. Sánchez, Electrical effects generated by mechanical loading of hardened Portland cement paste, Cem. Concr. Compos. 25 (3) (2003) 351–356, https://doi.org/10.1016/S0958-9465(02)00053-7.

[49] J.M. Ortega, I. Sánchez, C. Antón, G. De Vera, M.A. Climent, Influence of environment on durability of fly ash cement mortars, ACI Mater. J. 109 (2012).

[50] C. Andrade, C. Alonso, A. Arteaga, P. Tanner, Methodology based on the electrical resistivity for the calculation of reinforcement service life, in: V.M. Malhotra (Ed.), Proc. 5th CANMET/ACI Int. Conf. Durab. Concr. Suppl. Pap., American Concrete Institute, Barcelona, Spain, 2000: pp. 899–915.

[51] ASTM, ASTM C642 - 06 Standard Test Method for Density, Absorption, and Voids in Hardened Concrete, (2006) 3.

[52] ASTM, ASTM C596 - 01 Standard Test Method for Drying Shrinkage of Mortar Containing Hydraulic Cement, (2001) 3.

[53] Jan Bijen, Benefits of slag and fly ash, Constr. Build. Mater. 10 (5) (1996) 309–314, https://doi.org/10.1016/0950-0618(95)00014-3.

[54] S. Sujjavanich, T. Meesak, D. Chayasuwan, Effect of clay brick powder on ASR expansion control of rhyolite mortar bar, 2014. 10.4028/www.scientific.net/AMR.931-932.441.